Journal of Solid State Chemistry 182 (2009) 2846–2851

Contents lists available at ScienceDirect

Journal of Solid State Chemistry

journal homepage: www.elsevier.com/locate/jssc

Crystal structure and electron density in the apatite-type ionic conductor $La_{9.71}(Si_{5.81}Mg_{0.18})O_{26.37}$

Roushown Ali [a,b,1], Masatomo Yashima [b,*], Yoshitaka Matsushita [a,2], Hideki Yoshioka [c], Fujio Izumi [a]

[a] Quantum Beam Center, National Institute for Materials Science, 1-1 Namiki, Tsukuba, Ibaraki 305-0044, Japan
[b] Department of Materials Science and Engineering, Interdisciplinary Graduate School of Science and Engineering, Tokyo Institute of Technology, 4259 Nagatsuta-cho, Midori-ku, Yokohama 226-8502, Japan
[c] Hyogo Prefectural Institute of Technology, 3-1-12 Yukihira-cho, Suma-ku, Kobe 654-0037, Japan

ARTICLE INFO

Article history:
Received 13 April 2009
Received in revised form
20 July 2009
Accepted 27 July 2009
Available online 4 August 2009

Keywords:
Apatite-type structure
Rietveld refinement
MEM analysis
Electron density distribution
Synchrotron X-ray powder diffraction

ABSTRACT

Crystal structure and electron density in the apatite-type ionic conductor $La_{9.71}(Si_{5.81}Mg_{0.18})O_{26.37}$ have been investigated at 302, 674 and 1010 K by Rietveld refinement and a whole-pattern fitting approach based on the maximum-entropy method (MEM) using synchrotron X-ray powder diffraction data. Second harmonic generation measurements indicated that the space group of this material is centrosymmetric. Among the possible hexagonal groups $P6_3/m$, $P6_3$ and $P\bar{3}$ the former is correct for $La_{9.71}(Si_{5.81}Mg_{0.18})O_{26.37}$. Rietveld refinements suggested an oxygen interstitial site (0.03,0.15,0.85) near the hexagonal axis. MEM analyses revealed that the $Si_{0.97}Mg_{0.03}$ atom has covalent bonds with four adjacent oxygen atoms to form a tetrahedron. The oxygen O4 atom located at the 2*a* site (0.0,0.0,1/4) exhibited large atomic displacement parameters along the *c* axis and electron density mapping also indicated the wide distribution consistent with migration of oxygen ions in this direction.

1. Introduction

Solid oxides that exhibit high ionic conductivity have attracted widespread interest in recent years owing to their technological importance in a number of applications, such as oxygen sensors, separation membranes and solid oxide fuel cells. It is well known that among many structural families, fluorite- and perovskite-type structures show higher oxide-ion conductivities and interesting structural properties [1–5]. The other family is of the apatite-type which has recently appeared as a new class of oxide ion conductors following the pioneering work of Nakayama et al. [6–8]. These materials take the general formula $A_{10-x}M_6O_{26+y}$ (where A = rare earths, alkaline earths; M = Si, Ge, P, V, etc). Among them, rare earth silicates and germanates are of particular interest because of their higher oxide ion conductivity.

The conductivity of the apatite-type lanthanum silicates can be increases with Mg substitution for Si [9–11]. It has also been reported [5,12–14] that the conductivity of the apatite-type systems is enhanced largely by the incorporation of excess oxygen where the number of oxygen atoms per formula unit is larger (O_{26+y}) than that of the oxygen stoichiometric composition O_{26}. The crystal structures of Mg-doped lanthanum silicates with stoichiometric O_{26} oxygen atoms, $La_{9.5}Si_{5.75}Mg_{0.25}O_{26}$ and $La_{9.67}Si_{5.5}Mg_{0.5}O_{26}$, have been studied by Kendrick et al. [9]. They reported the space group to be hexagonal $P6_3$ and suggested the presence of a small level of interstitial oxygen at the periphery of hexagonal channel close to the silicon groups through the difference Fourier maps, but they did not succeed in the refinement of the positional parameters of the oxygen atoms in their Rietveld analysis. Yoshioka [10,11] studied the ionic conductivity of Mg-doped lanthanum silicates with excess oxygen atoms $La_{9.6}Si_{5.8}Mg_{0.2}O_{26.1}$ and $La_{10}Si_{6-x}Mg_xO_{27-x}$ and reported that the composition at $x = 0.3$ has the highest conductivity at 1073 K, but, the structural details are not satisfactorily understood. Based on the analogous composition reported in the literature the excess interstitial was assumed to reside in $P6_3/m$ without crystal structure refinement. Therefore, the space group and position of the interstitial site must be clear. Furthermore, no study on electron density distribution of these apatite-type ionic conductors has yet been published.

The purpose of the present study is to determine the crystal structure with correct space group and to investigate the electron density distribution of $La_{9.71}(Si_{5.81}Mg_{0.18})O_{26.37}$ using second-harmonic-generation (SHG) measurements, Rietveld refinement [15,16] and the maximum-entropy method (MEM) [17–19]. This is followed by MEM-based pattern fitting (MPF) [19,20] of synchrotron X-ray powder diffraction data measured at 302, 674 and 1010 K. MEM-based pattern fitting (MPF) can be very effective for

* Corresponding author.
E-mail address: yashima@materia.titech.ac.jp (M. Yashima).
[1] Permanent address: Department of Chemistry, University of Rajshahi, Rajshahi 6205, Bangladesh.
[2] Present address: Beam line BL15XU, SPring-8, NIMS—Branch Office, 1-1-1 Kohto, Sayo-cho, Hyogo 679-5148, Japan.

0022-4596/$ - see front matter © 2009 Elsevier Inc. All rights reserved.
doi:10.1016/j.jssc.2009.07.053

determining precise electron density distributions that visualizes covalent bonding as we reported [21–27] for many compounds with different types of structure.

2. Experimental procedure

A $La_{9.71}Si_{5.81}Mg_{0.18}O_{26.37}$ sample was prepared by solid-state reaction from high-purity powders of La_2O_3, SiO_2 and MgO previously dried at 1273 K for 4 h. The powders were mixed in appropriate ratios, ground with ethanol and calcined at 1573 K for 16 h. The calcined powders were further ground, pressed into disks and sintered at 1873 K for 4 h in air. The first sintering gave porous disks because of high reactivity of the calcined powders with the atmospheric H_2O and CO_2. They were thus reground, pressed into disks and sintered again at 1823 K for 8 h on MgO-stabilized ZrO_2 setters placed inside a $MoSi_2$ furnace, resulting in dense ceramic disks with a diameter of ~13 mm and a thickness of ~1 mm. One of the sintered disks was crushed and ground into a powder for use in laboratory-based and synchrotron X-ray powder diffraction measurements. Inductively coupled plasma optical emission spectroscopy chemical analyses indicated that the chemical formula of the final product was $La_{9.71(1)}(Si_{5.81(1)}Mg_{0.18(1)})O_{26.37(2)}$ where the number in parenthesis is the error in the last digit. The value for oxygen 26.37 was calculated to achieve charge neutrality. The SHG measurement was done by the powder method with a Nd:YAG laser operating at a wavelength of 1064 nm, which was used as the radiation source with an irradiation time of 8 s. The laser power was 300 μJ. The sample was ground to a grain size of 1–2 μm in order to avoid the possible influence of domain structure and phase-matching conditions.

Synchrotron X-ray powder diffraction data were collected on a powder diffractometer installed at beam line 19B2 of SPring-8, Japan, with the Debye–Scherrer geometry. The wavelength of the monochromatized X-rays was determined to be 0.49952 Å using the NIST SRM silicon powders. The $La_{9.71}Si_{5.81}Mg_{0.18}O_{26.37}$ sample was loaded into a quartz-glass capillary tube with an inner diameter 0.3 mm and the tube rotated at 60 rpm during the measurements to minimize preferred-orientation and large-grain effects. The diffraction data were measured at 302, 674 and 1010 K over a 2θ range from 0.01° to 78.13° with a step interval of 0.01°. The sample temperature was calibrated with a thin thermocouple.

Table 1
Refined structural parameters of the $La_{9.71}(Si_{5.8}Mg_{0.2})O_{26.37}$, SG $P6_3/m$ (No.176).

Temperature		302 (K)	674 (K)	1010 (K)
Atom, Site, Occupancy	Structural parameters			
La1	x	1/3	1/3	1/3
4f	y	2/3	2/3	2/3
g(La1) = 0.927	z	−0.0006(2)	−0.0006(2)	−0.0004(2)
	U (Å^2)	0.0131(2)	0.0199(2)	0.0273(2)
La2	x	0.01128(10)	0.01110(10)	0.01136(10)
6h	y	0.23998(7)	0.23894(7)	0.23932(7)
g(La2) = 1.0	z	1/4	1/4	1/4
	U (Å^2)	0.0100(2)	0.0166(2)	0.0224(2)
$Si_{0.97}Mg_{0.03}$	x	0.4031(3)	0.4037(3)	0.4031(3)
6h	y	0.3732(3)	0.3737(3)	0.3738(3)
g(Si) = 0.970	y	1/4	1/4	1/4
g(Mg) = 0.030	U (Å^2)	0.0070(7)	0.0137(7)	0.0181(7)
O1	x	0.3237(7)	0.3244(7)	0.3252(7)
6h	y	0.4883(7)	0.4883(6)	0.4884(6)
g(O1) = 1.0	z	1/4	1/4	1/4
	U (Å^2)	0.018(2)	0.021(2)	0.029(2)
O2	x	0.5971(7)	*0.5959(6)*	0.5952(6)
6h	y	0.4757(7)	0.4731(6)	0.4724(6)
g(O2) = 1.0	z	1/4	1/4	1/4
	U (Å^2)	0.008(1)	0.016(2)	0.022(2)
O3	x	0.3467(5)	0.3441(4)	0.3428(4)
12i	y	*0.2566(4)*	*0.2578(4)*	*0.2577(4)*
g(O3) = 1.0	z	0.0714(5)	0.0709(5)	0.0708(4)
	U_{11} (Å^2)	*0.056(4)*	*0.067(3)*	*0.079(3)*
	U_{22} (Å^2)	0.006(4)	0.022(3)	0.030(3)
	U_{33} (Å^2)	*0.010(3)*	*0.017(3)*	*0.017(3)*
	U_{12} (Å^2)	*0.019(3)*	0.030(3)	*0.035(3)*
	U_{13} (Å^2)	−0.020(2)	−0.020(2)	−0.022(2)
	U_{23} (Å^2)	−0.014(2)	−0.014(2)	−0.015(2)
	U_{eq} (Å^2)	0.024	0.032	0.039
O4	x	0	0	0
2a	y	0	0	0
g(O4) = 1.0	z	1/4	1/4	1/4
	U_{11} (Å^2)	0.026(5)	0.028(5)	0.033(5)
	U_{33} (Å^2)	0.186(15)	0.189(14)	0.200(13)
	U_{eq} (Å^2)	0.079	0.082	0.089
O5	x	0.102(6)	0.080(10)	0.094(9)
12i	y	0.162(5)	0.142(9)	0.144(8)
g(O5) = 0.031	z	0.811(9)	0.852(13)	0.834(13)
	U (Å^2)	0.006	0.013	0.013

Number of the formula in a unit cell, $Z = 1$.

The synchrotron X-ray powder diffraction data were analyzed by the Rietveld method followed by application of MEM-based pattern fitting (MPF) [19,20] using the computer programs RIETAN-FP [28] and PRIMA [29]. A split-type pseudo-Voigt profile function formulated by Toraya [30] was used in the Rietveld refinements. A Legendre polynomial function with 12 parameters was fitted to background intensities. Isotropic atomic displacement parameters (U) including the isotropic Debye–Waller factor ($= \exp(-8\pi^2 U \sin^2\theta/\lambda^2)$) were assigned to all cation and O1, O2, O5 sites (Table 1), and anisotropic atomic displacement parameters (U_{ij}) with the anisotropic Debye–Waller factor ($= \exp[-2\pi^2(h^2a^{*2}U_{11}+k^2b^{*2}U_{22}+l^2c^{*2}U_{33}+2hka^*b^*U_{12}+2hla^*c^*U_{13}+2klb^*c^*U_{23})]$) were assigned to O3 and O4 sites.

3. Results and discussion

All the reflections of the Mg doped lanthanum silicate $La_{9.71}Si_{5.81}Mg_{0.18}O_{26.37}$ compound at 302, 674 and 1010 K were indexed by a hexagonal cell (for example $a = 9.7203(2)$ and $c = 7.20045(9)$ Å at 302 K, Fig. 1). In accordance with earlier reports the rare earth silicates and germanates belong to hexagonal space group $P6_3/m$, $P\overline{3}$ or $P6_3$. The $P6_3/m$ and $P\overline{3}$ space groups have center of symmetry while $P6_3$ does not have. In the apatite-type materials, the deformation in the $P\overline{3}$ and $P6_3$ structures from the $P6_3/m$ symmetry is small and all the three space groups can index all the peaks in the diffraction profiles. To determine the correct space group, it is important to examine the center of symmetry of the compounds. Therefore, we carried out SHG measurement for $La_{9.71}(Si_{5.81}Mg_{0.18})O_{26.37}$, which is a powerful method [31,32] to test the absence of a symmetry center in the compound. From this measurement, we obtained no evidence of SHG, which confirmed that $La_{9.71}(Si_{5.81}Mg_{0.18})O_{26.37}$ compound has center of symmetry. Therefore, the non-centrosymmetric space group $P6_3$ can be ruled out for $La_{9.71}(Si_{5.81}Mg_{0.18})O_{26.37}$, which has been reported for $La_{9.5}Si_{5.75}Mg_{0.25}O_{26}$ and $La_{9.67}Si_{5.5}Mg_{0.5}O_{26}$ [9]; $La_{9.33}Si_6O_{26}$ and $La_9AESi_6O_{26+y}$ (AE = Ba, Sr and Ca) [33]; $La_{9.83}Si_{4.5}Co_{1.5}O_{26}$, $La_{9.66}Si_5CoO_{26}$, $La_{10}Si_5CoO_{26.5}$ and $La_8BaCoSi_6O_{26}$ [34]; and $La_{9.67}Si_5GaO_{26}$ [35]. The SHG measurement proved that $La_{9.71}(Si_{5.81}Mg_{0.18})O_{26.37}$ compound does not belong to non-centrosymmetric $P6_3$. Therefore, it belongs to centrosymmetric space group $P6_3/m$ or $P\overline{3}$.

An important difference between $P6_3/m$ and $P\overline{3}$ space groups is that $P\overline{3}$ generates extra 0 0 1 reflection at 3.98° in 2θ compared to $P6_3/m$. In the diffraction pattern no peak is observed at that position, which suggests that the compound belongs to $P6_3/m$. But since 0 0 1 reflection generated by $P\overline{3}$ could extremely be weak and there was no effect of this reflection in the Rietveld profile fitting results for the synchrotron X-ray diffraction data. Therefore, we refined the crystal structure of $La_{9.71}(Si_{5.81}Mg_{0.18})O_{26.37}$ with both the space groups $P6_3/m$, and $P\overline{3}$. The unit-cell parameters obtained from the synchrotron X-ray powder diffraction

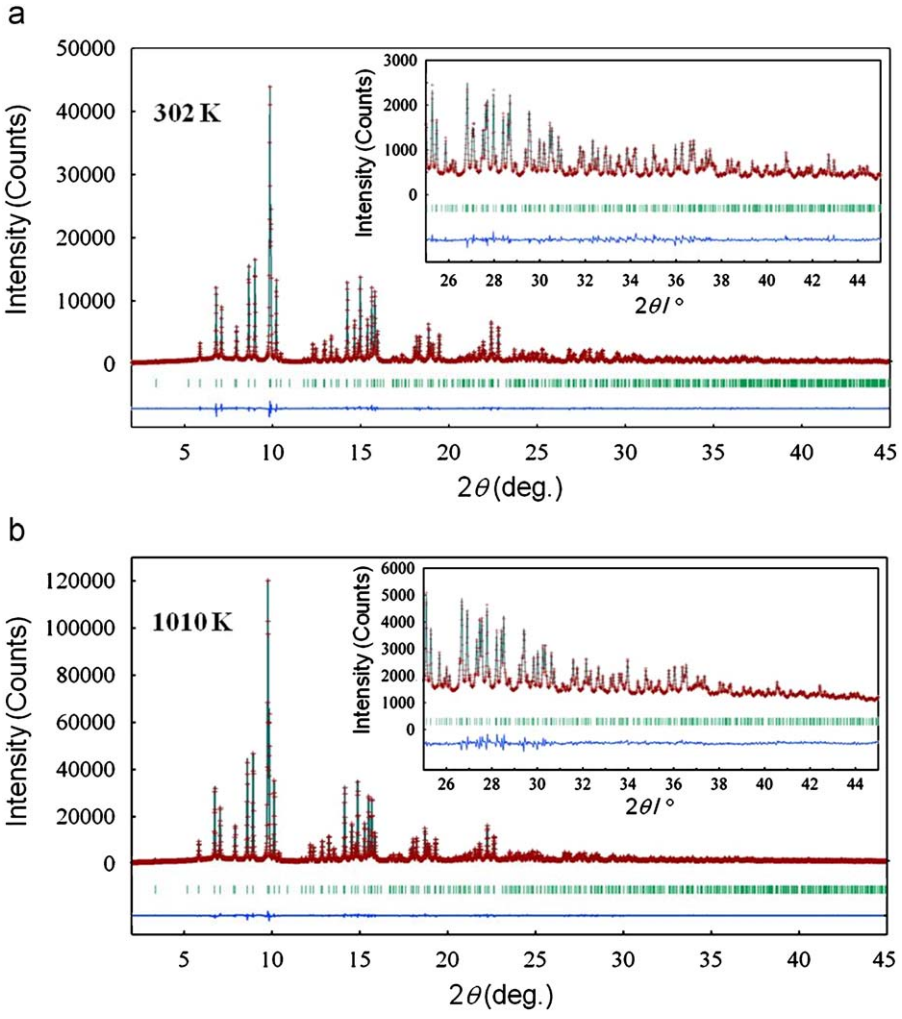

Fig. 1. Rietveld fitting pattern for $La_{9.71}(Si_{5.81}Mg_{0.18})O_{26.37}$ at (a) 302 K and (b) 1010 K. Crosses and lines denote observed and calculated profile intensities, respectively. Short vertical bars represent Bragg reflection positions. The difference (observed–calculated) is plotted below each profile.

data measured at 302 K were $a = 9.7203(2)$, $c = 7.20045(9)$ Å and $a = 9.72018(9)$, $c = 7.20037(5)$ Å for $P6_3/m$, and $P\bar{3}$, respectively, which are very close to each other. The reliability indices based on the weighted profile R_{wp} were 3.88% and 3.76% for $P6_3/m$ and $P\bar{3}$, respectively. These profile fitting results are also fairly close, although the reliability indices of $P\bar{3}$ were slightly lower compared to $P6_3/m$. The slightly improved fit obtained from $P\bar{3}$ (23 structural parameters) is attributable to the difference in number of refined structural parameters compared to $P6_3/m$ (15 parameters). Hence, the slightly improved fitting obtained from $P\bar{3}$ is not significant and we concluded that $La_{9.71}(Si_{5.81}Mg_{0.18})O_{26.37}$ is $P6_3/m$. This space group was also reported for non-doped lanthanum silicates [36–41] and doped (on Si site) lanthanum silicates $La_{9.33+x/3}(SiO_4)_{6-x}(AlO_4)_xO_2$ $(0 \le x \le 2)$, [42] $La_{9.33}(Si_{3.0}Ge_{3.0})O_{26}$, [38] $(La_{9.33}(Si_{5.7}Mg_{0.3})O_{26.1}$, [10] $La_{9.71}(Si_{4.86}Mg_{1.14})O_{26}$, [42] and $La_{9.69}(Si_{5.70}Mg_{0.30})O_{26.24}$ [43]. We have given for the first time direct evidence for a center of symmetry in the $La_{9.71}(Si_{5.81}Mg_{0.18})O_{26.37}$ through the SHG measurements.

In a preliminary analysis, the site occupancies of La atoms at the La1 (x, 1/3, 2/3; $x \sim 0.927$) and La2 (x, y, 1/4; $x \sim 0.011$, $y \sim 0.24$) sites, g(La1) and g(La2) were refined, which resulted in non-physical value (g(La2) > 1.0). Consequently, the occupancy factor of g(La2) was fixed at 1.0 in the subsequent refinements. Simultaneously, g(La1) was fixed at 0.927 to satisfy the chemical composition. Attempts to refine the occupancy factor of O4 atom located at (0.0, 0.0, 1/4) gave higher value than unity, thus it was fixed at unity in the whole temperature range. The Si and Mg atoms were assumed to occupy the same site and occupancies of the atoms were fixed at the values of the chemical composition.

In $P6_3/m$, $La_{9.71}(Si_{5.81}Mg_{0.18})O_{26.37}$ has O1, O2, O3, O4 atoms and the interstitial oxygen O5. The oxygen composition 26.37(2) estimated from chemical analysis indicates 0.37(1) interstitial per unit cell. In preliminary refinements, attempts to put (i) the extra oxygen at different positions at (0, 0, z) on the hexagonal axis, (ii) a split-atom model for O4 at 4e site (0, 0, z), instead of 2a (0, 0, 1/4), and (iii) placing a small amount of oxygen on 4e site together with 2a site, were unsuccessful. Subsequently, we placed the extra oxygen (O5) at an interstitial site (12i; (x, y, z)) near the hexagonal channel proposed from atomistic simulation studies for the space group $P\bar{3}$ [44,45] and neutron diffraction studies [38,40] for $P6_3/m$. The 12i site ($x \approx 0.0$, $y \approx 0.15$, $z \approx 0.85$) accompanied by slightly improved reliability indices were obtained from the refinement with interstitial oxygen for all the temperatures. The improved profile fit supports the presence of the interstitial site (O5). The atomic displacement parameters of the O5 atom g(O5) were not refined because of the small occupancy, and was fixed at 0.013 for all the refinements. The Rietveld refinements revealed no oxygen vacancy on the hexagonal axis (2a site) and only the excess oxygen (O_y in $La_{9.71}(Si_{5.81}Mg_{0.18})O_{26+y}$) was assumed to occupy the interstitial site in the refinements.

Some preliminary refinements were performed using isotropic thermal displacement parameters for all the atoms that yielded large atomic displacement parameters for O3 and O4 atoms, but when the anisotropic atomic displacement parameters were refined for two anion sites, the profile fitting was superior.

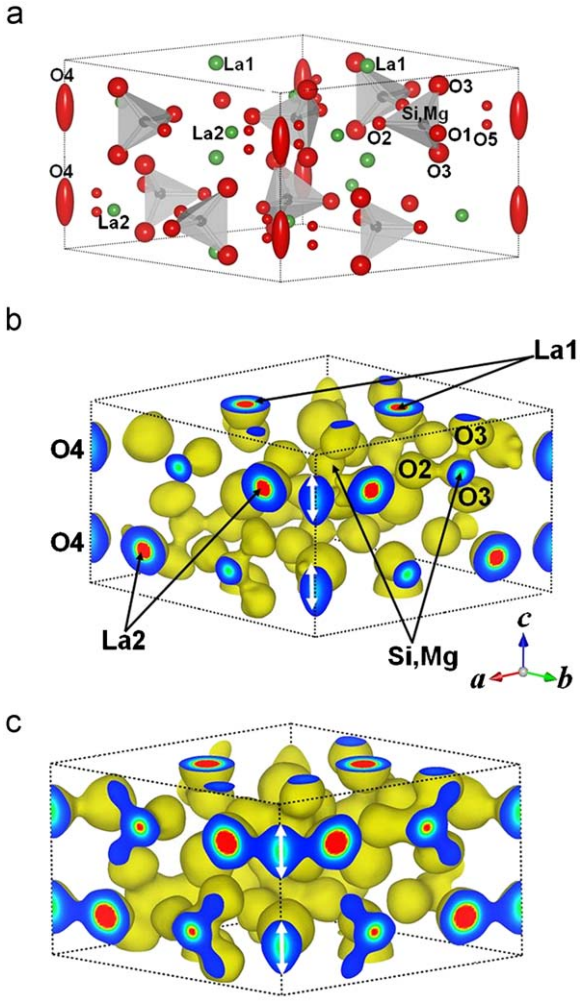

Fig. 2. (a) Refined crystal structure at 302 K. Equielectron density surfaces at 1.0 Å^{-3} of apatite-type $La_{9.71}(Si_{5.81}Mg_{0.18})O_{26.37}$ at (b) 302 K and at (c) 1010 K. O4 atoms have large distribution along the ⟨001⟩ direction (white arrows).

Table 2
Refined unit-cell parameters, reliability indices and metaprism twist angle of the $La_{9.71}(Si_{5.8}Mg_{0.2})O_{26.37}$, SG $P6_3/m$ (No. 176).

Temperature	302 (K)	674 (K)	1010 (K)
Unit-cell parameters			
a (Å)	9.7203(2)	9.7566(2)	9.7905(2)
c (Å)	7.20045(9)	7.21751(9)	7.23641(10)
Unit-cell volume (Å^3)	589.18(2)	594.99(2)	600.71(2)
Metaprism angle (deg)	21.47	21.84	21.85
Reliability indices[a]	$R_{wp} = 3.88\%$, $R_p = 2.98\%$ Goodness of fit = 1.23 $R_I = 1.36\%$, $R_F = 0.80\%$	$R_{wp} = 3.32\%$, $R_p = 2.52\%$ Goodness of fit = 1.66 $R_I = 1.28\%$, $R_F = 0.95\%$	$R_{wp} = 3.01\%$, $R_p = 2.26\%$ Goodness of fit = 1.54 $R_I = 1.45\%$, $R_F = 1.39\%$
Reliability indices[b]	$R_I = 0.99\%$, $R_F = 0.66\%$ ($N = 1$)	$R_I = 1.06\%$, $R_F = 0.82\%$ ($N = 1$)	$R_I = 1.19\%$, $R_F = 1.20\%$ ($N = 1$)

[a] Reliability indices in the Rietveld analysis.
[b] Reliability indices in the Nth MEM-based pattern fittings.

Refinements with anisotropic displacement parameters for cations and other oxygen atom sites resulted in no significant improvement in fit. Thus, anisotropic atomic displacement parameters, U_{ij}, were assigned only to O3 and O4 atoms in the final refinement, and the calculated profiles agreed well with observed intensities (Fig. 1). The atomic displacement parameter of O3 was anisotropic along the *a* axis, while that of O4 showed strong anisotropy along the *c* axis with larger U_{33} values (Table 1), suggesting that the atoms migrate to nearest-neighbor (O4) along the [001] direction. This anisotropic behavior increased with temperature, and is consistent with previous studies [36,38,39, 42–46]. The unit-cell parameters, unit-cell volume, metaprism twist angle and reliability indices for all the temperatures are listed in Table 2. The unit-cell parameters and volume at 302 K are consistent with that reported for $La_{9.5}Si_{5.75}Mg_{0.25}O_{26}$ [9] and $La_{9.6}Si_{5.7}Mg_{0.3}O_{26.1}$ [10], and increased with temperature. The unit-cell volume expanded linearly with temperature. The metaprism twist angles showed a little trend of increase with increasing temperature. This increase may be induced by thermal effect which rotates the angle of upper and lower pair of oxygen of the same metaprism. Positional parameters (Table 1) of all atoms were almost unchanged with temperature, except the oxygen atoms of the interstitial site. The *x* coordinate of the interstitial O5 atom increased a little while the *z* coordinate decreased with increasing temperature (Table 1). The *y* coordinate of O5 atom did not change so much with temperature.

The MEM analyses were performed using 804 structure factors obtained from the Rietveld analyses. By measuring the peak intensity of the 1 0 0 reflection at $2\theta \sim 3.4^{\circ}$, significant information about disordered arrangements of oxide ions is obtained. The MEM calculations were done using PRIMA [29] with the unit cell divided into $100 \times 100 \times 80$ pixels and whole-pattern fitting using RIETAN-FP [28]. To reduce the bias imposed on electron density by the simple structural model adopted in the Rietveld analyses, an iterative procedure named REMEDY cycle [20,29] was employed after the MEM analyses. Use of the REMEDY cycle resulted in significant improvement in the reliability indices based on the Bragg intensities (R_I) and structure factors (R_F) (Table 2). Electron-density images obtained after the REMEDY cycle were drawn with VESTA program [47] and are shown in Fig. 2(b, c) to visualize the density distribution derived from the MEM calculations.

Electron-density images indicate that oxide ions located at the hexagonal axis (O4) have wide distribution along 〈001〉 (white arrows in Fig. 2 (b, c)). The Rietveld refinement also indicated large anisotropic atomic displacement along 〈001〉 direction for these oxide ions (Table 1). The directionality in the electron

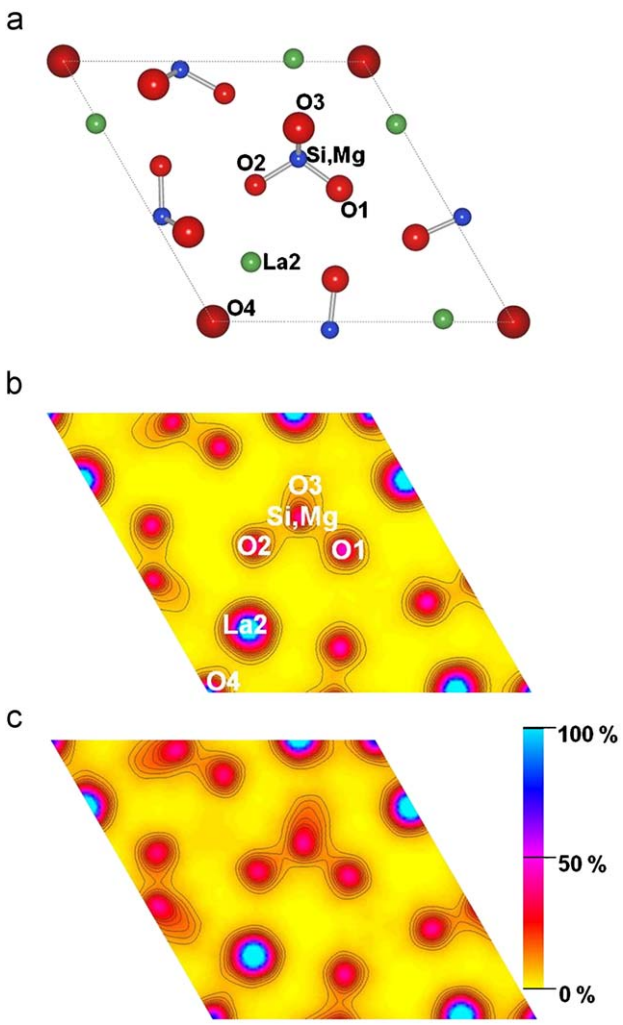

Fig. 3. (a) Refined crystal structure at 302 K, O5 atoms have been deleted in the atomic model. Electron density distribution on the (001) plane ($0.822 \leq z \leq 0.83$) of apatite-type $La_{9.71}Si_{5.81}Mg_{0.18}O_{26.37}$ at (b) 302 K and (c) 1010 K, with the black contours in the range from 0.9 to 4.0 $Å^{-3}$ (0.2 $Å^{-3}$ step). 100% of the scale (by color) corresponds to the electron density value of 16.4 $Å^{-3}$.

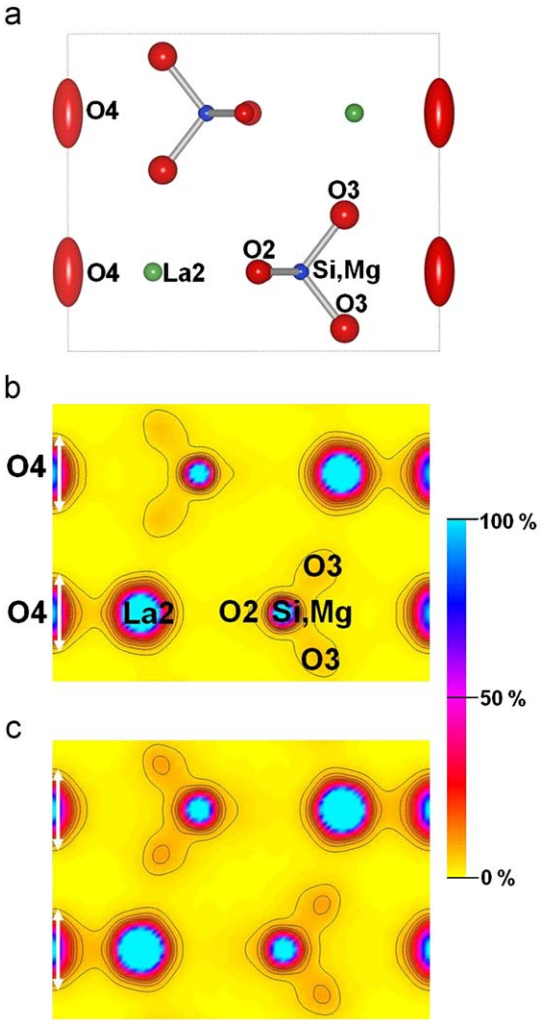

Fig. 4. (a) Refined crystal structure at 302 K, O5 atoms have been deleted in the atomic model. Electron density distribution on the (010) plane ($0.0 \leq z \leq 0.005$) of apatite-type $La_{9.71}Si_{5.81}Mg_{0.18}O_{26.37}$ at (b) 302 K and (c) 1010 K, with the black contours in the range from 0.5 to 4.0 $Å^{-3}$ (0.4 $Å^{-3}$ step). 100% of the scale (by color) corresponds to the electron density value of 16.4 $Å^{-3}$.

density distribution and the atomic displacement of the O4 atom, suggests a possible diffusion pathway where the oxide ions migrate along the *c* axis. This result is in agreement with many structural studies of lanthanum silicates [36,37,40,43,45,46].

The electron density maps ((b, c) Figs. 2–4) clearly show that the $(Si_{0.97}Mg_{0.03})O_4$ tetrahedra have covalent character that might be formed by the overlap of Si 3p and O 2p electrons. In Fig. 2 (b, c) non-zero equielectron density surface between Si and O atoms indicate the covalent bonding between them. The minimum density of the Si–O bonds is 1.1 $Å^{-3}$ (on average) at 302 K. The electron density distributions obtained at different temperatures are not so different in shape, except a large thermal effect which probably expands the density distribution with temperatures.

The electron density distributions ((b, c) of Figs. 2, 3 and 4) suggests covalent bonding between the La2 and O4 atoms, which form by the overlap of La 5d and O 2p electrons. The minimum electron density of the La2–O4 bond was estimated to be 0.77 $Å^{-3}$ at 302 K. In comparison with the La2, the La1 atom is more isolated and ionic (Fig. 2 (b, c)).

We reported diffusion path of oxide ions in apatite-type $La_{9.69}(Si_{5.70}Mg_{0.30})O_{26.24}$ using neutron powder diffraction data in our recent published paper.[43] Similar diffusion path way and crystal structure we have observed with synchrotron X-ray powder diffraction for $La_{9.71}(Si_{5.81}Mg_{0.18})O_{26.37}$ in the present manuscript. In this work we have reported covalent bonding character among Si–O and La–O at different temperatures in apatite-type $La_{9.71}(Si_{5.81}Mg_{0.18})O_{26.37}$ with electron density distribution determined by maximum-entropy method (MEM). For this compound we have carried out second harmonic generation (SHG) experiment for the first time and established the space group on the basis of SHG result and Rietveld refinements.

Acknowledgments

The authors would like to thank the authority of SPring-8 for use of the beam line 19B2. Special thanks are extended to Mr. Takahiro Wakita, Mr. Qi Xu, Mr. Takayuki Tsuji and Mr. Yoichi Kawaike for experimental assistance. The authors thank Dr. M. Nakamura and Mr. S. Takenouchi (NIMS) for their help with SHG and ICP measurements, respectively. This research was supported in part by the Ministry of Education, Culture, Sports, Science and Technology of Japan (Monbu-Kagaku-sho).

References

[1] J.C. Boivin, G. Mairesse, Chem. Mater. 10 (1998) 2870.
[2] M. Yashima, D. Ishimura, Appl. Phys. Lett. 87 (2005) 221909.
[3] T. Ishihara, H. Matsuda, Y. Takita, J. Am. Chem. Soc. 116 (1995) 3801.
[4] M. Yashima, K. Nomura, H. Kageyama, Y. Miyazaki, N. Chitose, K. Adachi, Chem. Phys. Lett. 380 (2003) 391.
[5] P.R. Slater, J.E.H. Sansom, J.R. Tolchard, Chem. Rec. 4 (2004) 373.
[6] S. Nakayama, H. Aono, Y. Sadaoka, Chem. Lett. 6 (1995) 431.
[7] S. Nakayama, M. Sakamoto, J. Euro, Ceram. Soc. 18 (1998) 1413.
[8] S. Nakayama, M. Sakamoto, M. Higuchi, K. Kodaira, M. Sato, S. Kakita, T. Suzuki, K. Itoh, J. Euro, Ceram. Soc. 19 (1999) 507.
[9] E. Kendrick, J.E.H. Sansom, J.R. Tolchard, M.S. Islam, P.R. Slater, Faraday Discuss. 134 (2006) 181.
[10] H. Yoshioka, S. Tanase, Solid State Ionics 176 (2005) 2395.
[11] H. Yoshioka, Chem. Lett. 33 (2004) 392.
[12] J.E.H. Sansom, P.A. Sermon, P.R. Slater, Solid State Ionics 176 (2005) 1765.
[13] P.R. Slater, J.E.H. Sansom, Solid State Phenom. 90-91 (2003) 195.
[14] A. Najib, J.E.H. Sansom, J.R. Tolchard, P.R. Slater, M.S. Islam, Dalton Trans. (2004) 3106.
[15] H.M. Rietveld, J. Appl. Crystallogr. 2 (1968) 65.
[16] F. Izumi, T. Ikeda, Mater. Sci. Forum 321-324 (2000) 198.
[17] D.M. Collins, Nature 298 (1982) 49.
[18] M. Sakata, M. Sato, Acta Crystallogr. Sect. A 46 (1990) 263.
[19] F. Izumi, R.A. Dilanian, Recent Res. Phys. 3 (2002) 699.
[20] F. Izumi, S. Kumazawa, T. Ikeda, W-Z Hu, A. Yamamoto, K. Oikawa, Mater. Sci. Forum 378-381 (2001) 59.
[21] M. Yashima, M. Tanaka, J. Appl. Crystallogr. 37 (2004) 786.
[22] M. Yashima, in: Proceedings of the International Conference on Solid–Solid Phase Transformations in Inorganic Materials, vol. 2, 2005, p. 493.
[23] M. Yashima, S. Tsunekawa, Acta Crystallogr. B62 (2006) 161.
[24] M. Yashima, K. Oh-Uchi, M. Tanaka, T. Ida, J. Am. Ceram. Soc. 89 (2006) 1395.
[25] M. Yashima, Q Xu, A. Yoshiasa, S. Wada, J. Mater. Chem. 16 (2006) 4393.
[26] M. Yashima, Y. Lee, K. Domen, Chem. Mater. 19 (2007) 588.
[27] M. Yashima, K. Ogisu, K. Domen, Acta Crystallogr. B 64 (2008) 291.
[28] F. Izumi, K. Momma, Solid State Phenom. 130 (2007) 15.
[29] F. Izumi, R.A. Dilanian, Recent Res. Dev. Phys. 3 (2002) 699.
[30] H. Toraya, J. Appl. Crystallogr. 23 (1990) 485.
[31] T. Hahn (Ed.), International Tables for Crystallography, vol. A, fourth ed., Kluwer Academic Publishers, 1996, p. 790.
[32] S.K. Kurtz, T.T. Perry, J. Appl. Phys. 39 (1968) 3798.
[33] S. Lambert, A. Vincent, E. Bruneton, S. Beaudet-Savignat, F. Guillet, B. Minot, F. Bouree, J. Solid State Chem. 179 (2006) 2602.
[34] J.R. Tolchard, J.E.H. Sansom, M.S. Islam, P.R. Slater, Dalton Trans. (2005) 1273.
[35] J.E.H. Sansom, J.R. Tolchard, P.R. Slater, M.S. Islam, Solid State Ionics 167 (2004) 17.
[36] Y. Masubuchi, M. Higuchi, T. Takeda, S. Kikkawa, Solid State Ionics 177 (2006) 263.
[37] H. Okudera, Y. Masubuchi, S. Kikkawa, A. Yoshiasa, Solid State Ionics 176 (2005) 1473.
[38] L. Leon-Reina, E.R. Losilla, M. Martınez-Lara, S. Bruque, A. Llobet, D.V. Sheptyakov, M.A.G. Aranda, J. Mater. Chem. 15 (2005) 2489.
[39] H. Yoshioka, J. Alloys Comp. 408–412 (2006) 649.
[40] L. Leon-Reina, E.R. Losilla, M. Martinez-Lara, S. Bruque, M.A.G. Aranda, J. Mater. Chem. 14 (2004) 1142.
[41] E.J. Abram, D.C. Sinclair, A.R. West, J. Mater. Chem. 11 (2001) 1978.
[42] V. Kahlenberg, H. Kruger, Solid State Sci. 6 (2004) 553.
[43] R. Ali, M. Yashima, Y. Matsushita, H. Yoshioka, K. Ohoyama, F. Izumi, Chem. Mater. 20 (2008) 5203.
[44] M.S. Islam, J.R. Tolchard, P.R. Slater, Chem. Commun. (2003) 1486.
[45] J.R. Tolchard, M.S. Islam, P.R. Slater, J. Mater. Chem. 13 (2003) 1956.
[46] [a] T. Iwata, K. Fukuda, E. Béchade, O. Masson, I. Julien, E. Champion, P. Thomas, Solid State Ionics 178 (2007) 1523;
[b] E. Béchade, O. Masson, T. Iwata, I. Julien, K. Fukuda, P. Thomas, E. Champion, Chem. Mater. 21 (2009) 2508.
[47] K. Momma, F. Izumi, J. Appl. Crystallogr. 41 (2008) 635.